

IL-6-elafin genetically modified macrophages as a lung immunotherapeutic strategy against *Pseudomonas aeruginosa* infections

Saadé Kheir,¹ Bérengère Villeret,¹ Ignacio Garcia-Verdugo,¹ and Jean-Michel Sallenave¹

¹INSERM U1152, Laboratoire d'Excellence Inflammex, Université de Paris, Hôpital Bichat—Claude-Bernard, Paris 75014, France

***Pseudomonas aeruginosa* (*P.a*) infections are a major public health issue in ventilator-associated pneumoniae, cystic fibrosis, and chronic obstructive pulmonary disease exacerbations. *P.a* is multidrug resistant, and there is an urgent need to develop new therapeutic approaches. Here, we evaluated the effect of direct pulmonary transplantation of gene-modified (elafin and interleukin [IL]-6) syngeneic macrophages in a mouse model of acute *P.a* infection. Wild-type (WT) or Elafin-transgenic (eTg) alveolar macrophages (AMs) or bone marrow-derived macrophages (BMDMs) were recovered from bronchoalveolar lavage or generated from WT or eTg mouse bone marrow. Cells were modified with adenovirus IL-6 (Ad-IL-6), characterized *in vitro*, and transferred by oropharyngeal instillation in the lungs of naive mice. The protective effect was assessed during *P.a* acute infection (survival studies, mechanistic studies of the inflammatory response). We show that a single bolus of genetically modified syngeneic AMs or BMDMs provided protection in our *P.a*-induced model. Mechanistically, Elafin-modified AMs had an IL-6-IL-10-IL-4R-IL-22-antimicrobial molecular signature that, in synergy with IL-6, enhanced epithelial cell proliferation and tissue repair in the alveolar unit. We believe that this innovative cell therapy strategy could be of value in acute bacterial infections in the lung.**

INTRODUCTION

Pseudomonas aeruginosa (*P.a*) is a pathogen causing significant morbidity and mortality, in particular in hospital patients undergoing ventilation and in patients with cystic fibrosis (CF).^{1,2} Treatment of lower respiratory tract *P.a* infections becomes particularly problematic since *P.a* is resistant to standard or reserve antibiotic therapy.³ Indeed, the most recent global priority list of antibiotic-resistant bacteria to guide research, discovery, and development of new antibiotics from the WHO describes carbapenem-resistant *P. aeruginosa* as one of the most critical pathogens for which new treatment options are urgently required.⁴ Our group has recently shown that *P.a*-derived Elastase B (LasB) downregulates a lung epithelial-interleukin (IL)-6-antimicrobial-repair pathway,⁵ which results in a stronger inflammatory response and a higher mortality rate in a murine model of *P.a* lung infection.

Therefore, we reasoned that overexpressing IL-6 and elafin, two main targets of LasB, may be beneficial against *P.a* lung infection and that the alveolar macrophage (AM)⁶ may be an ideal vessel for the transfer of this protective activity. Indeed, compared to the direct instillation of viral vectors, a cell therapy approach has the advantage of being immunologically relatively “silent” and has indeed successfully been used in severe combined immunodeficiency (SCID) patients, where lymphocytes and stem cells have been efficiently corrected using lentiviruses.^{7,8} Crucially, adenovirus (Ad)-vectors offer the advantage, over other vectors such as lentiviruses, of remaining episomal in the nucleus and therefore not requiring integration into host chromosomes to deliver their genetic cargo.⁹

Importantly, AMs represent the most abundant myeloid cells in alveolar spaces.^{10,11} They are critical regulators in the maintenance of immunologic homeostasis¹¹ in the respiratory tract and play a key role in the initiation and resolution of the immune response in the lungs.^{12,13} Surprisingly, given their importance, few studies have focused on immunotherapy approaches involving direct pulmonary macrophage transplantation. Notably, in a mouse model of hereditary pulmonary alveolar proteinosis (hPAP) characterized by a disruption of the granulocyte-macrophage colony-stimulating factor (GM-CSF) receptor gene *Csf2*, the disease was corrected after the administration of wild-type (WT) macrophages directly in the lungs.¹⁴ Also, a recent study has shown that intra-pulmonary transplantation of bioreactor-derived induced pluripotent stem cell-macrophages (iPSC-Macs) rescues mice from *P.a*-mediated acute infections of the lower respiratory tract.¹⁵

Here, we demonstrate that the transfer in the lung of a single bolus of syngeneic AMs or bone marrow-derived macrophages (BMDMs) genetically modified with adenovirus IL-6 (Ad-IL-6) and Elafin provided protection in our *P.a*-induced model. Mechanistically, we demonstrate that prior to transfer the Elafin-modified AM had an “IL-6/IL-10/IL-4R/IL-22/antimicrobial” molecular signature that, in synergy with

Received 30 January 2021; accepted 29 July 2021;
<https://doi.org/10.1016/j.ymthe.2021.08.007>.

Correspondence: Jean-Michel Sallenave, INSERM U1152, Laboratoire d'Excellence Inflammex, Université de Paris, Hôpital Bichat—Claude-Bernard, Paris 75014, France.

E-mail: jean-michel.sallenave@inserm.fr



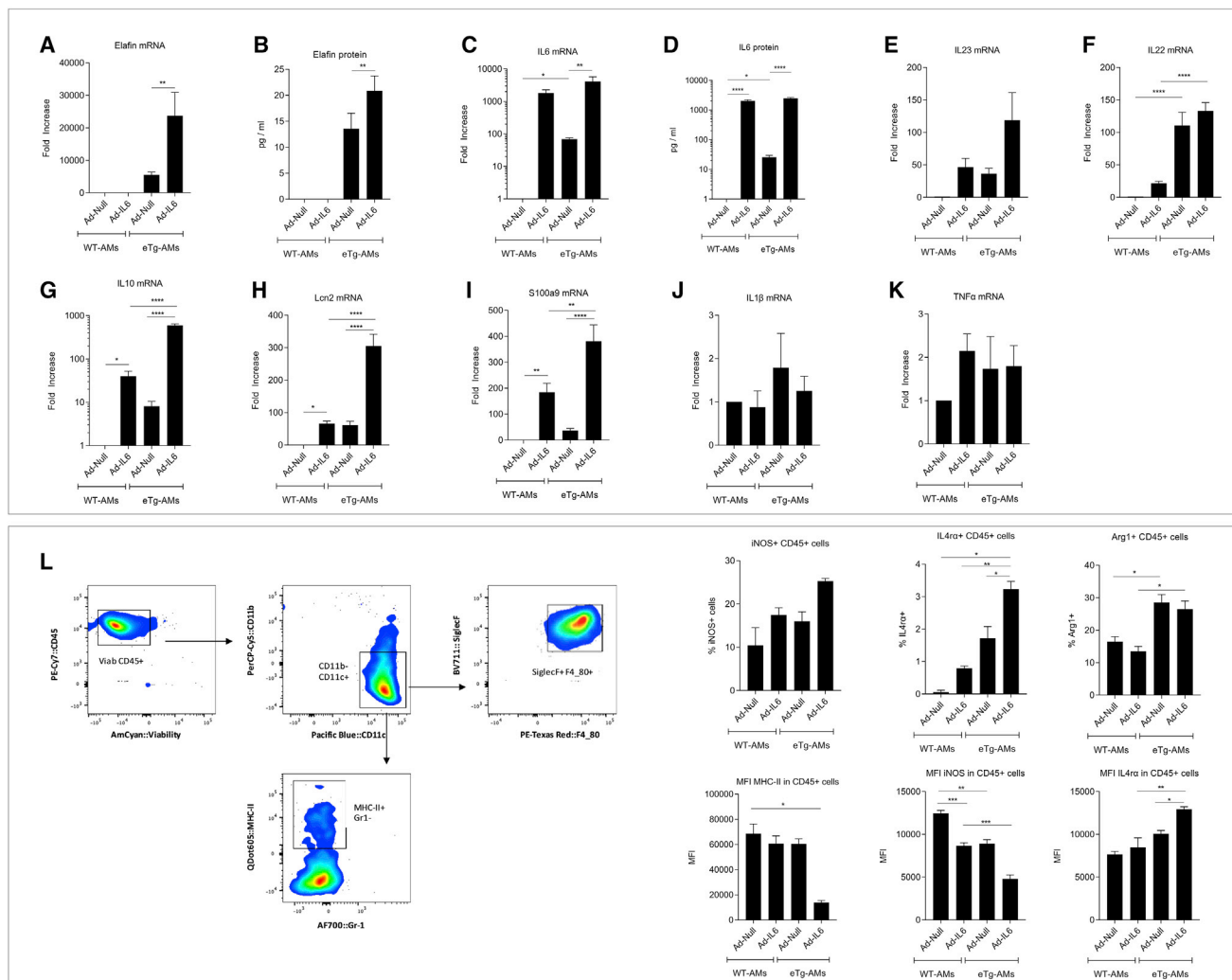


Figure 1. Elafin and IL-6 modify the transcriptional profile and polarization of alveolar macrophages

(A–K) WT or elafin transgenic (eTg) primary alveolar macrophages (WT-AMs or eTg-AMs) recovered from mice BALs were transfected for 6 h with adenovirus (MOI 25) Ad Null or Ad-IL-6 and left overnight. Supernatants were then used for IL-6 and elafin protein level measurements (ELISA). In parallel, cells were then lysed and the cell lysates were used for mRNA quantification by qPCR according to the $\Delta\Delta Ct$ method, with relative expression (fold increase) = $2^{-\Delta\Delta Ct}$. The relative expression, normalized to the housekeeping gene 18 s, of elafin, cytokine, and antimicrobial peptide mRNA as well as IL-6 and elafin protein levels in supernatants (measured by ELISAs) are presented. Fold changes are normalized to the WT Ad Null condition, which is considered 1. Data show mean \pm SEM ($n = 4$ independent experiments). Statistical significance: ANOVA, multiple comparison, Tukey's test, * $p < 0.05$; ** $p < 0.01$; *** $p < 0.001$; **** $p < 0.0001$. (L) WT-AMs and eTg-AMs were recovered by BALs as above and were washed with FACS buffer (PBS-FCS 1%) for FACS staining with a viability dye and fluorochrome-conjugated antibodies against the surface markers CD45, CD11b, CD11c, Gr-1 (Ly6c, Ly6G), MHC-II, F4/80, and SiglecF. A representative panel of AM markers is represented. Histograms represent % of cells iNOS+, Arg-1+, and IL-4+r+ and mean fluorescence intensity (MFI) FACS values. Statistical significance is as above.

IL-6, conferred, after transfer, a regulatory phenotype (decrease in iNOS, increase in Arg-1, Ym-1, IL-4Ra, IL-10) and an increase in type I-to-type II alveolar epithelial cell ratio, as well as a rise in proliferative markers.

RESULTS

IL-6 and elafin overexpression modifies cytokine and antimicrobial peptide production and the polarization profile of AMs

Unsurprisingly, as previously demonstrated,¹⁶ the elafin protein is not expressed in WT C57BL/6 mice and was only detected in pri-

mary AMs of elafin transgenic (eTg) mice (Figures 1A and 1B). In uninfected AMs, furthermore, elafin and IL-6 were shown to up-regulate each other: macrophages from eTg mice (eTg-AMs) have higher IL-6 levels at steady state (Figures 1C and 1D) and macrophages transfected with adenovirus (Ad-) overexpressing IL-6 (Ad-IL-6) upregulated elafin expression in eTg-AMs (Figures 1A and 1B).

Mechanistically, the positive effect of elafin on IL-6 expression was explained by the ability of the elafin to enter the nucleus, bind

DNA, and interact with the IL-6 promoter (see corresponding [Figures S1–S2](#) and [Supplemental Results](#)).

In addition, elafin and IL-6 modified the AM transcriptional profile. Indeed, we show that WT and eTg primary AMs are inherently different: the latter have higher basal levels of the antimicrobial peptides Lcn2 and S100a9 ([Figures 1H](#) and [1I](#)) as well as of the cytokines IL-23 ([Figure 1E](#), trend), IL-10, and IL-22 ([Figures 1F](#) and [1G](#)). Moreover, Ad-IL-6 enhances these differences by upregulating the expression of these mediators, especially Lcn2, S100a9, and IL-10 ([Figures 1G–1I](#)). Demonstrating specificity, IL-6 and/or Elafin have no effect on IL-1 β and tumor necrosis factor alpha (TNF- α) expression ([Figures 1J](#) and [1K](#)).

In addition to the classical AM markers, which did not differ between WT and eTg mice (presence of CD11c, SiglecF, and F4/80 and absence of Ly6C and Ly6G [not shown]), a small, nevertheless significant proportion of AMs (10%) expressed the major histocompatibility complex (MHC)-II molecule. Importantly, elafin and IL-6 expression polarized AMs toward an M2 profile, as demonstrated by an increase in Arg-1+ and IL-4 α + cell percentage ([Figure 1L](#)). Furthermore, elafin and Ad-IL-6 expression in eTg-AMs significantly downregulated MHC-II and iNOS mean fluorescence intensity (MFI) levels while upregulating those of IL-4 α .

Adoptive transfer of IL-6- and elafin-genetically modified AMs protects mice against *Pseudomonas aeruginosa*

250,000 primary WT AMs or eTg-AMs were then transfected with Ad Null or Ad-IL-6 and transferred by oropharyngeal instillation into naive male C57BL/6 mice, and bronchoalveolar lavages (BALs) were performed 2 days after transfer ([Figure 2A](#)). Compared to controls, all adoptive transfer groups had higher numbers of cells in BAL fluid (BALF) ([Figure 2B](#)) and exhibited a macrophagic CD11c+ phenotype ([Figure 2C](#)), without any neutrophilic infiltrate ([Figure 2D](#)). Interestingly, the MHC-II marker was significantly diminished in the eTg-AM + Ad-IL-6 transferred group, suggesting an M2 profile ([Figure 2C](#)).

Echoing *in vitro* data ([Figure 1](#)), IL-6 protein levels were higher in BALs from eTg-AMs + Ad Null BMDM-transferred mice ([Figure 2E](#)). Also, expectedly, Ad-IL-6 infection significantly increased IL-6 levels in both groups, but the latter were even higher in the eTg-AM group ([Figure 2E](#)).

Having demonstrated that these adoptively transferred AMs had retained features of an M2 profile (downregulation of MHC-II) and were able to produce higher levels of IL-6 *in situ*, we analyzed these cells after *Pseudomonas aeruginosa* O1 (PAO1) infection, both *in vitro* and *in vivo*. *In vitro*, although the differences between WT and eTg-AMs were expectedly somewhat attenuated, given the “dominant” stimulus conferred by PAO1 infection, some important differences were still noted: IL-23 mRNA and Lcn-2 mRNA levels were still upregulated by IL-6 ([Figures 3A5](#) and [3A8](#)) and were maximal in eTg-AMs, and S100A9 levels were higher in eTg-AMs

([Figure 3A9](#)), compared to WT AMs, in the absence of IL-6 stimulation. Interestingly, confirming the “M2/regulator” character of the genetically modified macrophages, this polarization did not enhance the capacity of primary AMs to clear PAO1 ([Figure 3B](#)) and even decreased the bactericidal activity of MPI (macrophage cell line) cells overexpressing elafin, alone or in conjunction with IL-6, as well as the production of reactive oxygen species (ROS) ([Figures 3C](#) and [3D](#)). Importantly, elafin and/or IL-6 overexpression also increased Lcn-2 and S100A9 responses in that cell line ([Figures S3G](#), [S3H](#), and [Supplemental results](#)).

Finally, when comparing the survival of WT C57BL/6 mice adoptively transferred with either AM-(WT+ Ad Null) or AM-(eTg + Ad-IL-6) (the two “extreme” conditions), we showed that the latter treatment significantly delayed mortality after a lethal dose of PAO1 ([Figure 3E](#)).

Adoptive transfer of IL-6- and elafin-genetically modified BMDMs protects mice against *Pseudomonas aeruginosa*

Because the total number of recoverable AMs is understandably limited (~120,000 per mouse), IL-6- and elafin-gene-modified BMDMs were then genetically modified as above and used in most of the rest of the study ([Figure 4A](#)).

Flow cytometry analysis of WT BMDMs showed that, in contrast to primary AMs that are CD11c+ Ly6C–, these cells are CD11b+ Ly6C–/+ ([Figure 4B](#)). As expected, they expressed the surface marker F4/80, which is a hallmark of macrophages, but not the alveolar residency marker SiglecF. A small proportion of BMDMs (~15%) were MHC-II+, and, as found in AMs ([Figure 2B](#)), fewer eTg-BMDMs expressed that marker, compared to WT BMDMs, with or without Ad-IL-6 infection ([Figure 4C](#)). Similarly to what was observed in AMs, IL-6 treatment, in conjunction with the expression of elafin, polarized BMDMs toward an M2 profile, as assessed by increased Arg-1+ and IL-4R α + and decreased iNOS+ cell frequencies ([Figure 4C](#)). Interestingly, the elafin-mediated IL-4R α induction was induced at least partly via endogenous IL-6, since an antibody against IL-6 significantly downregulated it (not shown).

As expected, *in vitro*, BMDMs produced increased levels of the pro-inflammatory cytokine IL-1 β after PAO1 infection ([Figures 5B7](#) and [5B8](#)), and, as shown earlier with primary AMs, basal or PAO1-induced expression of IL-6 was higher in eTg BMDMs than in WT-BMDMs ([Figure 5B2](#)).

Further, an adoptive transfer of BMDMs (mock treated or genetically modified) followed by a lethal PAO1 infection showed that >50% of mice in the eTg-AdIL6-BMDM group survived and were able to recover their initial body weight ([Figure 5C](#)).

In an independent experiment stopped before the death of mice (16 h after PAO1 administration, [Figure S4A](#)), fluorescence-activated cell sorting (FACS) analysis of BALs containing unmodified BMDMs at day 3 after transfer showed two distinct cell populations ([Figure S4B](#)).

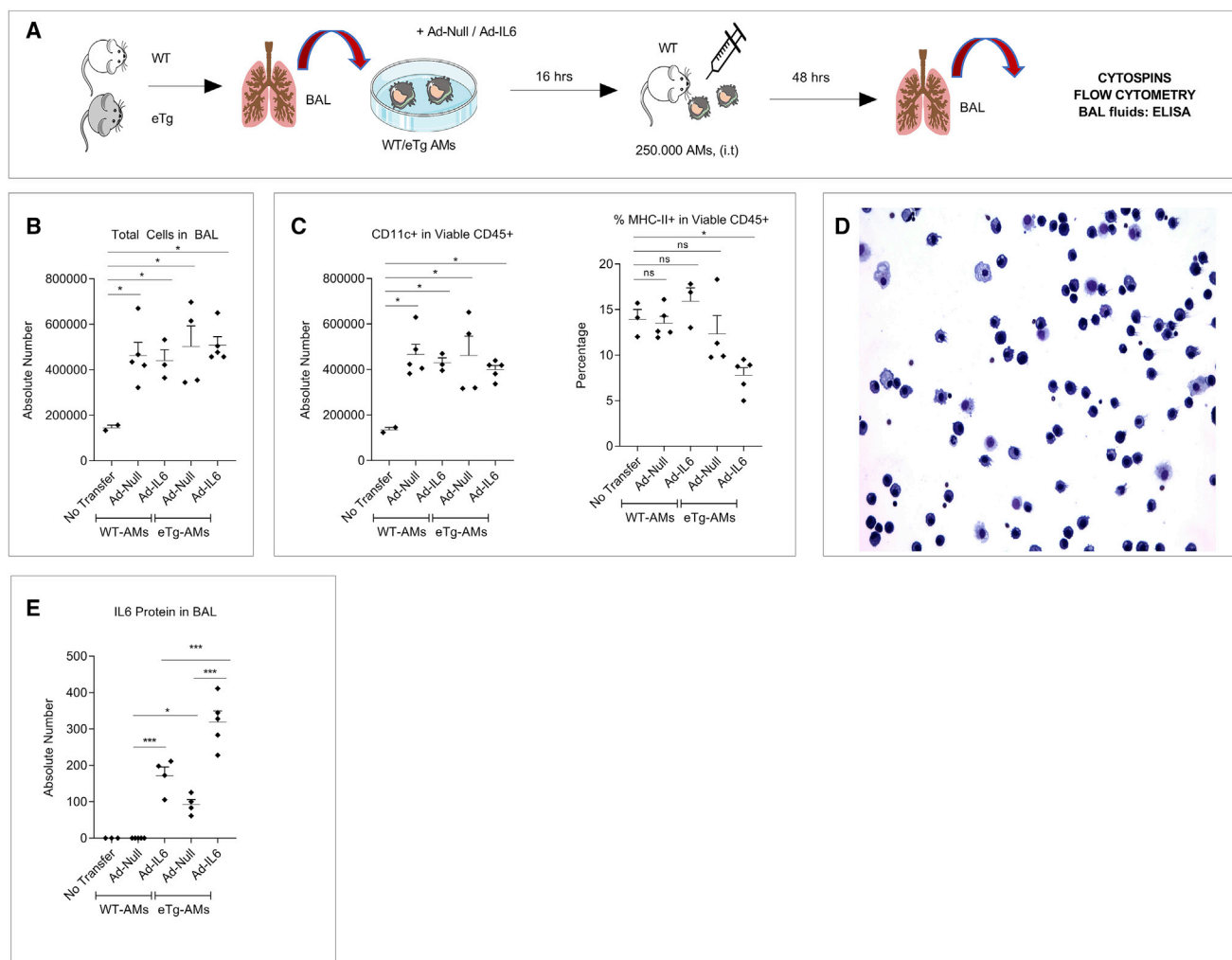


Figure 2. *In situ* characteristics of eTg-AdIL6 AMs adoptively transferred in the lungs of WT C57BL/6 mice

(A) Experimental procedure: Primary alveolar macrophages (WT-AM or eTg-AM) recovered by BAL were infected for 6 h with adenovirus (MOI 25) Ad Null (Control, CTRL) or Ad-IL-6 and left overnight. The next day, cells were detached with PBS-EDTA 0.5 mM and washed and the cell pellet was re-suspended in sterile PBS for adoptive transfer. 250,000 AMs were adoptively transferred in each C57BL/6 mouse through the oropharyngeal route. (B and D) 48 h after transfer, a BAL was performed and cells were counted (B), cytopsin, and stained with the MGG Diff-Quik staining kit; a representative BAL is shown (D). (C) Flow cytometry analysis of BAL cells from adoptively transferred mice: CD11c and MHC-II expression in viable CD45+ cells BAL cells is plotted. (E) Protein levels of IL-6 in BALF supernatants are plotted. Each point represents an individual mouse. Data show mean \pm SEM. Statistical significance: ANOVA, multiple comparison, Tukey's test, * $p < 0.05$; ** $p < 0.01$; *** $p < 0.001$; **** $p < 0.0001$.

CD11c+ cells (17%) were likely resident AMs (since they are Ly6C⁻, Ly6G⁻, F4-80⁺, and SiglecF⁺), whereas CD11b+ cells (the majority, 73%) most probably represented the BMDMs transferred at day 0. Interestingly, however, the latter became SiglecF^{+/-} intermediate (possibly through the influence of local lung cues) and acquired the Ly6G markers, becoming double positive for Ly6C and Ly6G, a hallmark of myeloid-derived suppressor cells.

After PAO1 infection (Figures S4B2 and S4C), there was, expectedly, a modulation of cell influx, as exemplified by an increase in BAL total cell numbers (Figure S4C1) in all groups, largely composed of neutrophil infiltrates (Figures S4B2 and S4C3) in the alveolar space. No

differences, however, were observed in cell population influx in the alveolar space (e.g., dendritic cells [DCs, Figure S4C2]) when experimental groups (WT versus eTg and WT+Ad-IL-6 versus eTg + Ad-IL-6) were compared with each other. However, iNOS⁺ cells, which were increased after PAO1 infection, remained low in the eTg-BMDM groups, with or without Ad-IL-6 treatment (Figure S4C4). Also, BALF IL-1 β , IL-6, and Lcn2 proteins were all induced equally in all groups after PAO1 infection (Figure S4D). Interestingly, compared to the WT-BMDM group, the eTg-BMDM group, which had fewer iNOS⁺ cells, had high IL-10 levels after PAO1 infection (Figure S4D4). This indicates that, in addition to low iNOS expression, eTg-BMDM transfer induced the production of high levels of

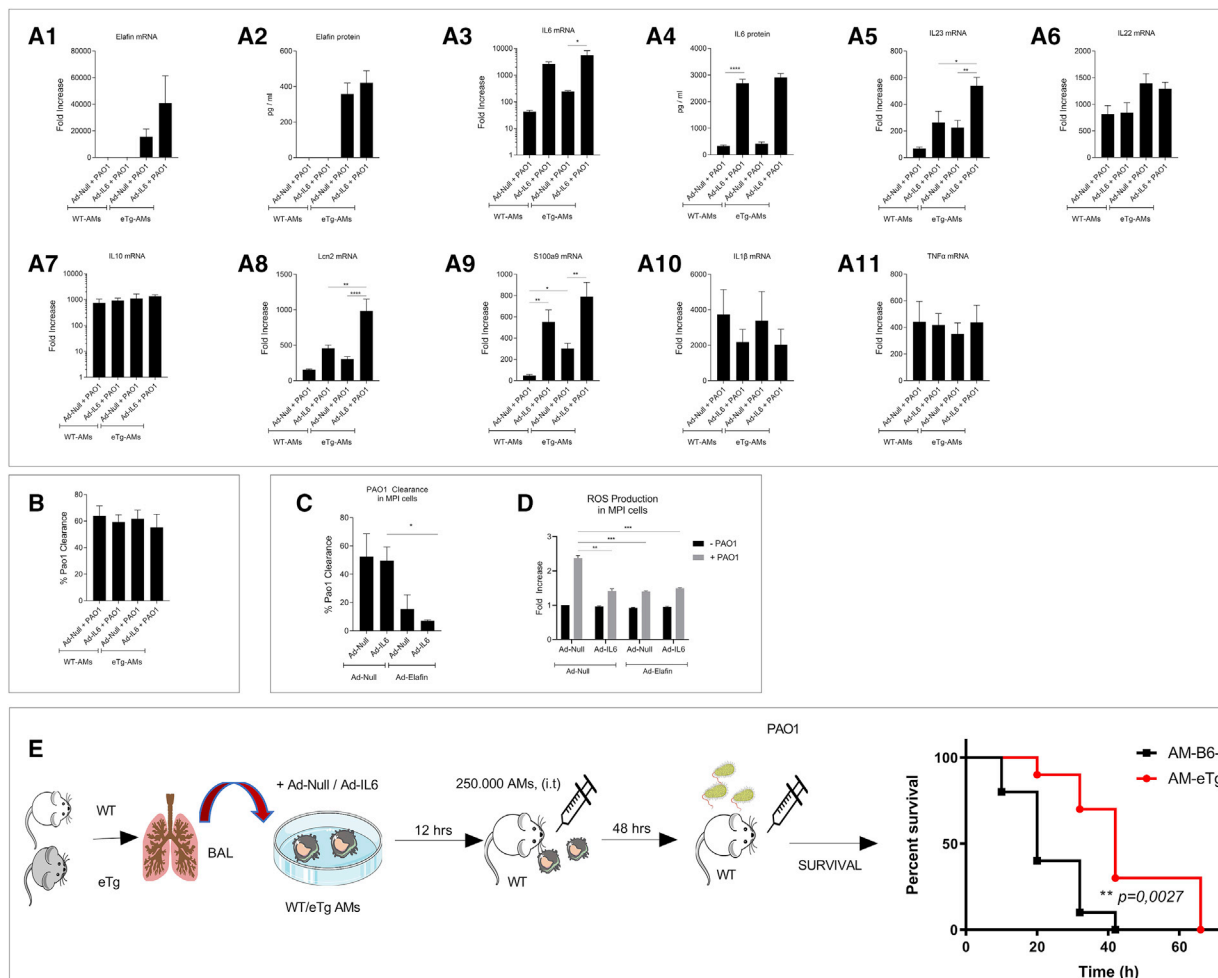


Figure 3. Lung adoptive transfer of eTg-AdIL6 AMs protects mice against lethal *Pseudomonas aeruginosa* (PAO1) infection

(A) WT or eTg primary alveolar macrophages (WT-AM or eTg-AM) recovered from mice BALs were transfected for 6 h with adenovirus (MOI 25) Ad Null or Ad-IL-6 and left overnight as in Figure 1. The next day, cells were washed and infected with WT PAO1 (MOI 0.5). After 4 h, supernatants and cell lysates were treated as in Figure 1. Fold changes are normalized to the WT Ad Null condition, which is considered 1. (B and C) In independent experiments, PAO1 clearance by WT-AMs or eTg-AMs was measured in WT-AMs and eTg-AMs (B) and in MPI cells by counting colonies on agar beads, as described in Materials and methods (C). (D) ROS production in MPI cells transfected with Ad Null or Ad-IL-6/elafin. Data show mean \pm SEM ($n = 4$ independent experiments). Statistical significance: ANOVA, multiple comparison, Tukey's test, * $p < 0.05$; ** $p < 0.01$; *** $p < 0.001$; **** $p < 0.0001$. (E) Adenovirus-transfected (but not PAO1 infected) WT/eTg-AMs (as in A) were transferred into male C57BL/6 mouse receivers. Animals were then infected 48 h later with 9×10^6 CFU PAO1/mouse. Survival was plotted with Kaplan-Meier curves, and statistical testing was performed with the log-rank (Mantel-Cox) test ($n = 10$ animals/group).

the regulatory/anti-inflammatory cytokine IL-10, suggesting that the high survival rate in this group (Figure 5) may be the consequence of a dampening of deleterious inflammatory responses. Importantly, neither IL-6 nor Elafin overexpression had an effect on PAO1 killing (Figure S4E).

Because IL-10 is a hallmark of a suppressive environment, we tested the BALF capacity to inhibit T cell proliferation. Carboxyfluorescein succinamide ester (CFSE)-loaded splenocytes were cultured with BALF recovered from the different groups analyzed in Figure S4. Flow cytometry analysis of CFSE expression (Figure S5) shows that BALF recovered from the group transferred with eTg-AdIL6-

BMDMs significantly inhibited splenocyte proliferation with or without PAO1 infection, confirming the presence of a suppressive and anti-inflammatory alveolar environment.

BMDM-mediated suppressive phenotype does not rely on T cells or innate-like lymphocytes

Because eTg-IL6-BMDMs are high *in situ* producers of IL-10 (Figure S4) and can condition a suppressive alveolar environment (Figure S5), we wondered whether BMDMs could interact *in situ* with “regulatory lymphocytes.” To that aim, we performed, as above, adoptive transfer experiments of genetically modified BMDMs in Rag1-gc double knockout (KO) mice. Importantly, after lethal

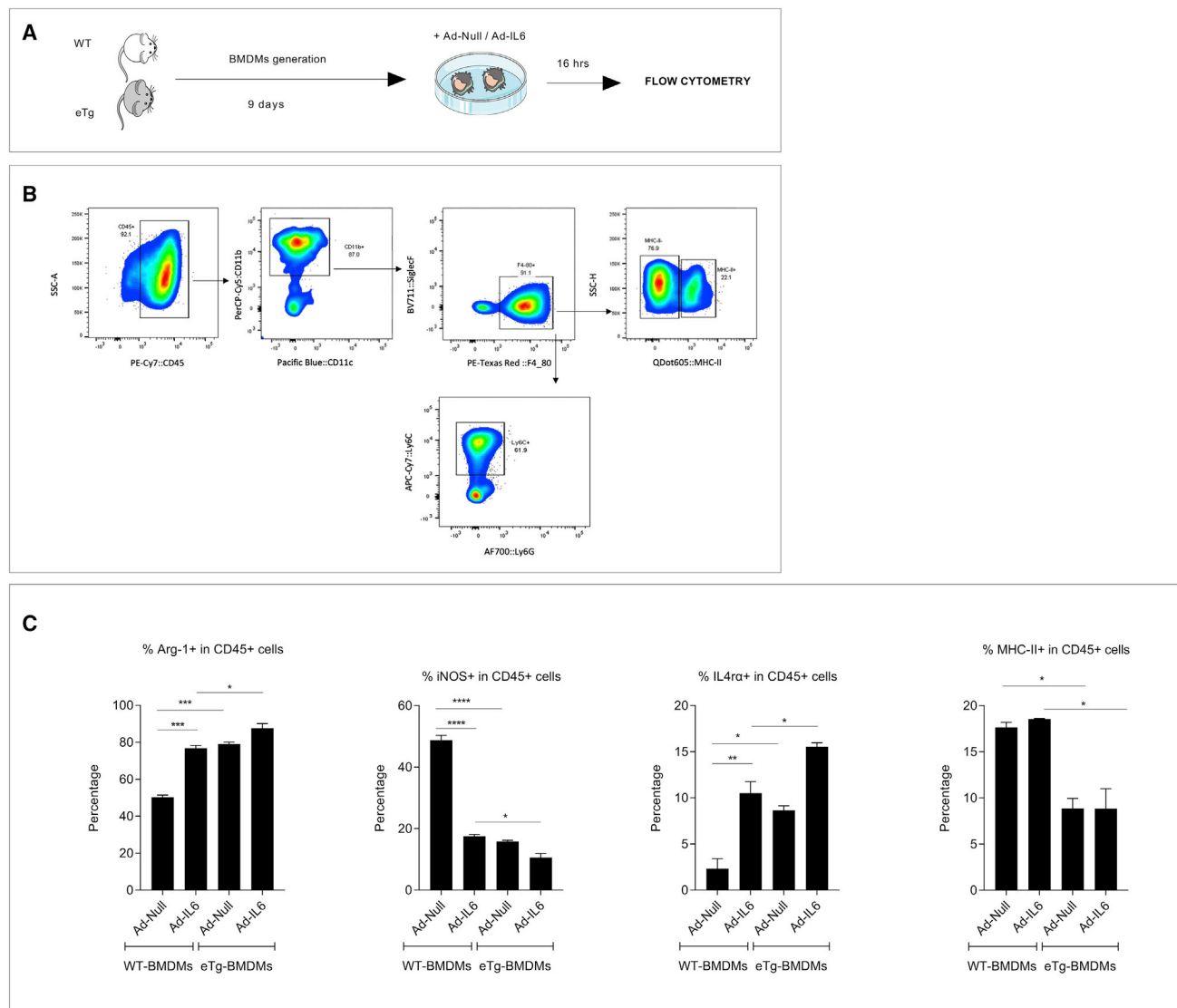


Figure 4. Flow cytometry analysis of BMDM markers: Elafin and IL-6 expression modify BMDM expression of Arg-1, iNOS, and IL-4 α markers

(A) Experimental procedure: WT and eTg-BMDMs were infected with Ad Null or Ad-IL-6 (MOI 25) and kept in culture for 16 h. The next day, cells were suspended in PBS-FCS 1% for FACS analysis. (B) FACS BMDM staining procedure using CD45, CD11b, CD11c, Gr-1 (Ly6c, Ly6G), MHC-II, F4/80, and SiglecF markers (a representative Ad Null treatment is depicted). (C) FACS study of BMDM polarization markers: the frequencies of iNOS-, Arg-1-, IL4 α -, and MHC-II-positive cells (among CD45+ viable cells) are depicted. Data show mean \pm SEM ($n = 3$ independent experiments). Statistical significance: ANOVA, multiple comparison, Tukey's test, * $p < 0.05$; ** $p < 0.01$; *** $p < 0.001$; **** $p < 0.0001$.

PAO1 infection, we showed that eTg + IL-6 transferred BMDMs still provided protection in that setup, demonstrating the latter to be independent of lymphocytes (Figure 6).

Adoptive transfer of IL-6- and elafin-genetically modified BMDMs induces a regulatory and repair phenotype in the alveolar space upon a sub-lethal PAO1 infection

To further dissect the molecular and cellular events involved here, we sacrificed mice 3 days after PAO1 (Figure 7A), a time point described as that of the onset of lung repair following *P.a* infection.¹⁷ We showed

(Figure 7B and Figure S6 for the gating strategy) that in PAO1-treated mice there was a decrease in type I (T-I) pneumocyte population, using podoplanin as a marker,^{18,19} consistent with PAO1-induced disruption of the epithelial barrier. Importantly, this decrease was less important in mice that received eTg-BMDMs and was completely rescued in mice transferred with eTg-AdIL-6 BMDMs (Figure 7B). Interestingly, there was no statistically significant loss of type II (T-II) pneumocytes after PAO1 infection (not shown), with instead a T-I-to-T-II ratio around 0.5 (Figure 7C), in accordance with the literature,²⁰ confirming that the T-II population is more resistant to injury-induced apoptosis.²¹

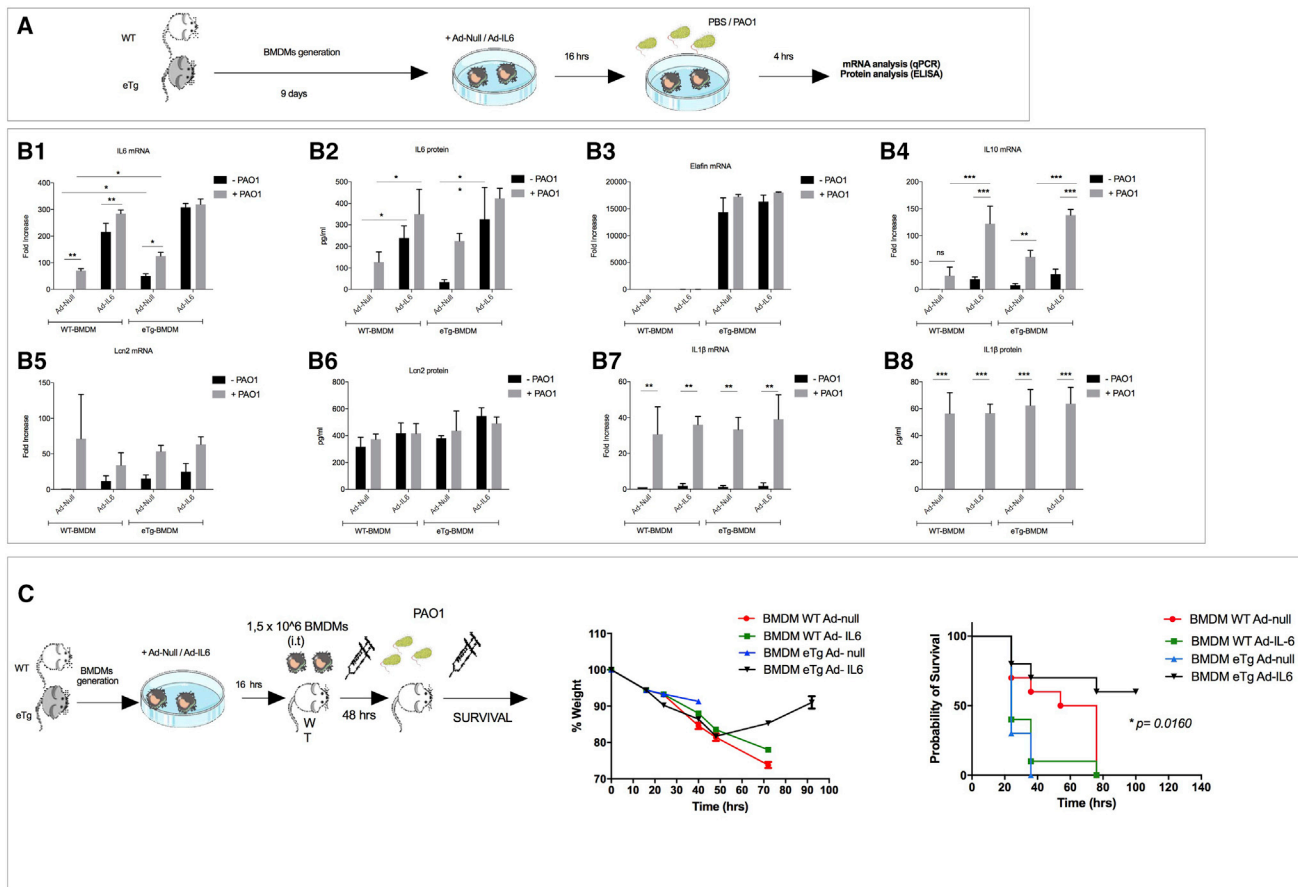


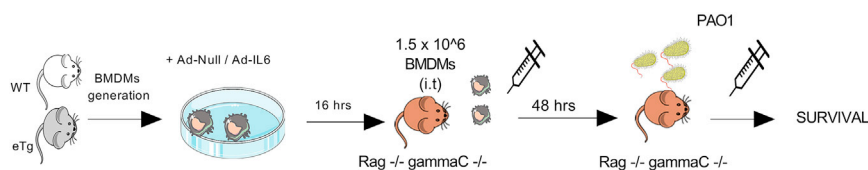
Figure 5. Elafin and IL-6 expression modify IL-10 BMDM output, and lung adoptive transfer of eTg-AdIL6 BMDMs protects mice against lethal PAO1 infection

(A and B) WT and eTg BMDMs were infected for 6 h with Ad Null or Ad-IL-6 (MOI 25) as above and infected with PAO1 (MOI 0.5) for 4 h. Then, IL-6, IL-10, IL-1β, Lcn2, and Elafin mRNA and protein levels were determined by qPCR and ELISA, respectively. Fold changes are normalized to the WT Ad Null (–PAO1) condition, which is considered 1. Data show mean ± SEM (n = 3 independent experiments). Statistical significance: ANOVA, multiple comparison, Tukey’s test, *p < 0.05; **p < 0.01; ***p < 0.001; ****p < 0.0001. (C) C57BL/6 WT male mice were transferred with 1.5 × 10⁶ WT/eTg BMDMs pre-infected with Ad Null or Ad-IL-6, as above. 48 h after transfer, mice were infected by intranasal route with 9 × 10⁶ CFU PAO1/mouse. Body weight loss and survival (Kaplan–Meier curve) were monitored until either animal death or total recovery of the remaining mice. Statistical testing was performed with the log-rank (Mantel–Cox) test (n = 10 animals/group).

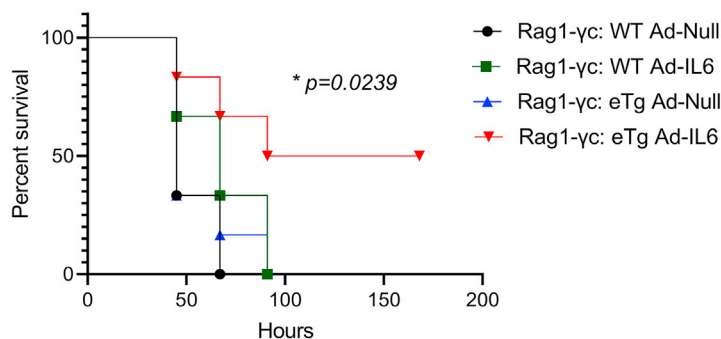
The contribution of IL-6-eTg combination to alveolar increased repair was further demonstrated with a t-distributed stochastic neighbor embedding (t-SNE) and self-organizing map (SOM) analysis (see [Materials and methods](#) for details). 70,000 random events, i.e., 8,750 per mouse × 4 mice × 2 groups (WT-Ad Null and eTg-IL-6) were analyzed with the tSNE script in FlowJo to create a 2-dimensional map ([Figure 7D](#)) and a heatmap of all the markers used in the experiment ([Figure 7E](#)). Further, 3 populations (Pops I–III) were identified whose frequencies were shown to be higher in the eTg-IL-6 group ([Figure 7F](#)). Finally, we focused on the bigger population (Pop I, [Figure 7G](#)), and a closer analysis of its markers revealed a high expression of EpCAM, Ki67, Podoplanin, and Sca-1 and a “mid” expression of SPC ([Figure 7H](#)). Importantly, Sca-1, a marker of alveolar type II proliferation, was significantly increased in mice transferred with eTg-BMDMs and still further in those given

eTg-IL-6 BMDMs ([Figure S7](#)). The enhanced interaction between BMDMs and epithelial cells was further confirmed in *in vitro* experiments in which eTg-IL-6 BMDMs enhanced the expression of antimicrobial and anti-inflammatory molecules in alveolar and Club epithelial cell lines (see corresponding [Figure S8](#) and [Supplemental results](#)).

Finally, we analyzed events at an even later time point. To that effect, mice were transferred with either WT-Ad Null or eTg-AdIL6 BMDMs (the two “extreme” experimental groups), infected with 5 × 10⁵ colony-forming units (CFU) of PAO1, and monitored for 5 days, until both groups recovered their original body weight ([Figures 8A](#) and [8B](#)). In that setup, differential characterization of BALF cells ([Figure 8B](#)) showed that the eTg-AdIL6-BMDM group had higher macrophage and lymphocyte numbers and fewer



Rag1-yc KO
BMDM WT vs BMDM eTg



neutrophils, suggesting a faster recovery process. Elafin mRNA expression in the alveolar cells of this group was increased, indicating that 7 days after BMDM transfer these cells still remained in the alveolar space (since WT C57BL/6 mice do not produce endogenous elafin), despite PAO1-mediated inflammation. Furthermore, ELISA dosage in BALF showed higher levels of IL-6, Lcn-2, Ym-1, and IL-10 in the eTg-IL-6-BMDM-treated groups, confirming a more efficient lung resolution and repair in this group (Figure 8C).

DISCUSSION

Although AM and epithelial cell pro-inflammatory activities are essential in the defense against pathogens,^{6,22,23} it is equally important that the alveolar unit maintain tolerogenic properties at homeostasis, before or after an infectious episode. Indeed, AMs and epithelial cells have been shown to interact closely and provide “anti-inflammatory signals” to the alveolar unit,^{11,24,25} and breaking that interaction was shown, for example, to induce emphysema in a murine model, through alteration of MMP-12 macrophage expression.²⁶

We show here that the transfer of a single bolus of syngeneic AMs or BMDMs genetically modified with IL-6 and elafin provided protection in a *P.a* lung infection murine model (Figure 3E and Figure 5C). Prior to transfer, eTg-BMDMs had a “IL-10/IL-4R” M2 regulatory signature compared to C57BL/6 WT mice (Figures 1, 2, 3, 4, and 5). This was associated with decreased MHC-II and ROS macrophage production (a hallmark of “M1 macrophages”) and, probably echoing the latter, a “neutral” or even a strong decrease (for MPI cells) in “direct” anti-PAO1 killing (Figures 3B–3D).

Figure 6. eTg-Ad-IL-6 BMDM-mediated regulatory phenotype does not rely on conventional or unconventional lymphocytes

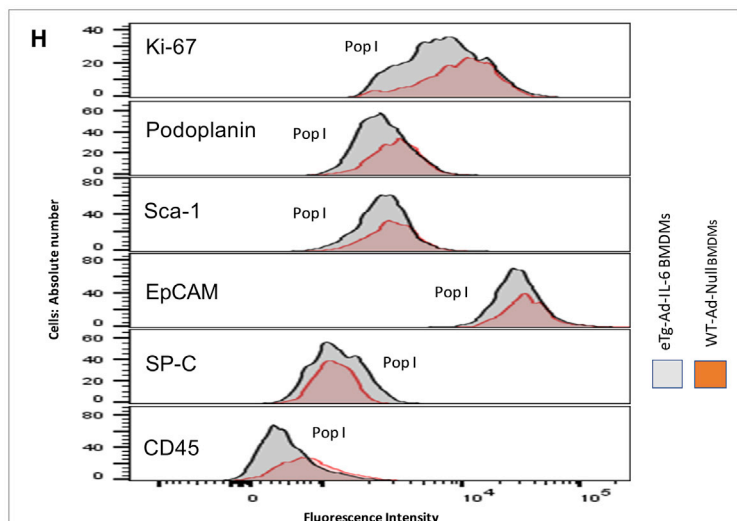
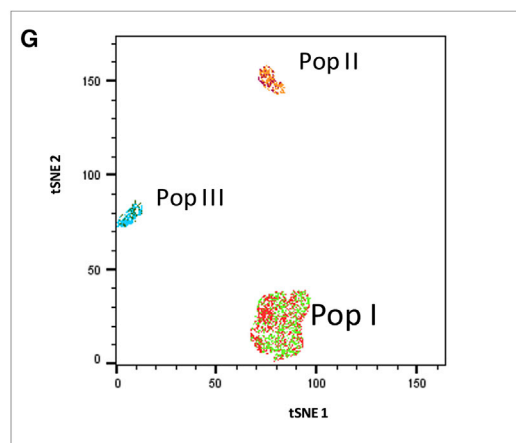
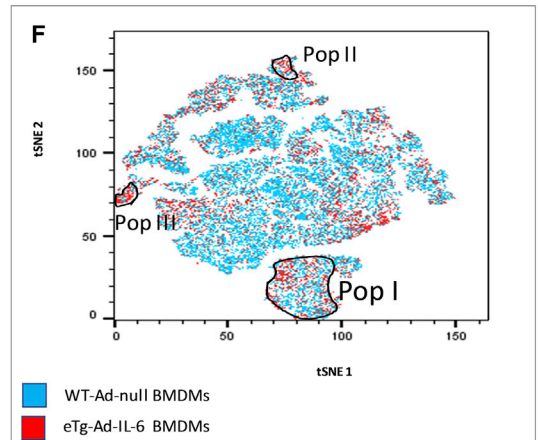
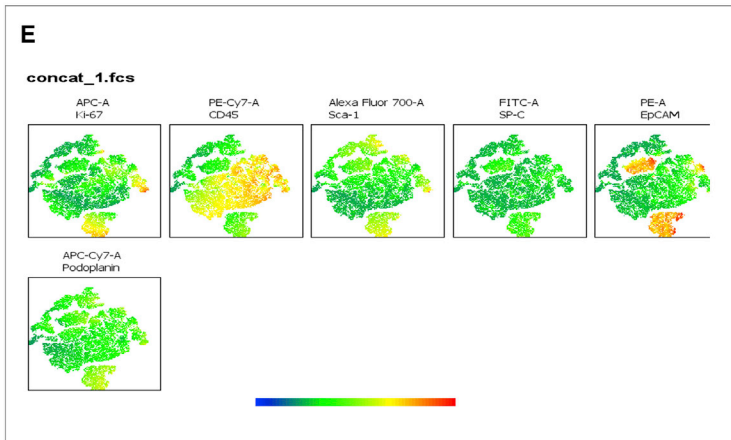
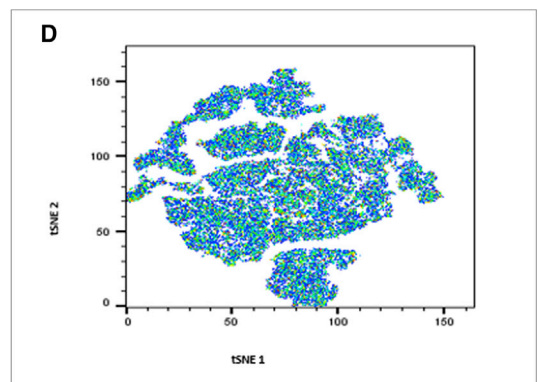
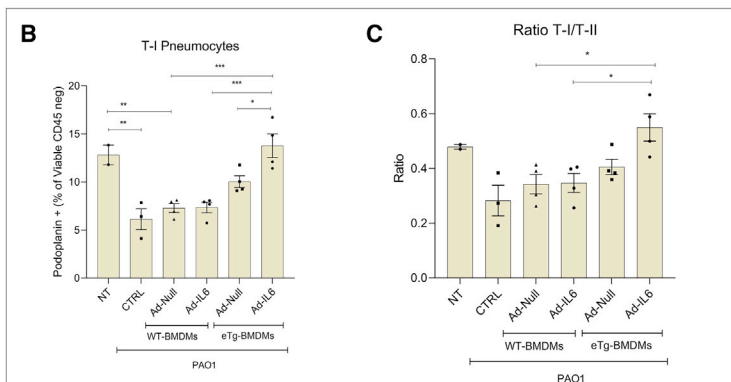
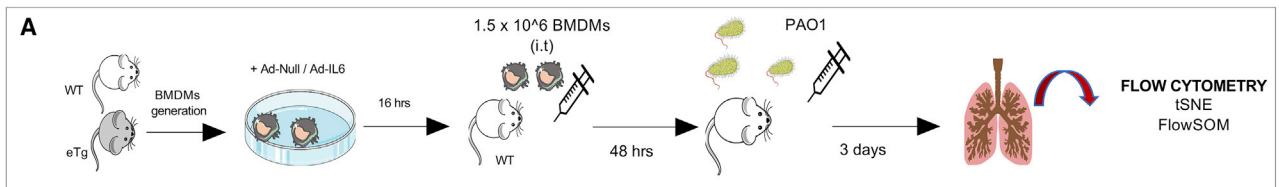
Rag gc double KO mice were transferred with 1.5×10^6 WT or eTg BMDMs pre-infected with Ad Null or Ad-mIL6 as above. 48 h after transfer, mice were infected intranasally with 1×10^7 WT PAO1 and survival was monitored until either animal death or total recovery of the remaining mice. Survival was plotted with Kaplan-Meier curves, and statistical testing was performed with the log-rank (Mantel-Cox) test ($n = 7$ animals/group).

This signature was reinforced when both elafin and IL-6 were associated, and, providing a potential explanation, we showed that these 2 mediators can upregulate each other’s expression and demonstrated for the first time, through independent methods, that elafin may get access to the nucleus and activate the IL-6 promoter (Figures S1, S2, and Supplemental results). This echoes previous studies indicating that secretory leucoprotease inhibitor (SLPI), a molecule with similar properties, was shown to cross the nuclear membrane thanks to its cationic properties and bind to nuclear factor κ B (NF- κ B) binding sites within the DNA.²⁷ IL-6 is the archetypical “pleiotropic cytokine,” able to promote either pro- or anti-inflammatory responses depending on the context.^{28,29} Reinforcing our data, it has been shown that IL-6 does not on its own bias immune responses but can, as shown here also, through the upregulation of the IL4R (Figures 2 and 4), enhance the action of IL-4, and hence a M2 phenotype.^{30–33}

Furthermore, the upregulation of IL-10 by elafin and IL-6 (Figures 1 and 5) is probably also instrumental in upregulating IL4R, since IL-10 was shown to be a potent inducer of IL-4Ra in a STAT-3-dependent fashion and in return, IL-4 could induce Arg-1 via STAT-6.³⁴

Notably, in addition to the “typical M2 markers” mentioned above, elafin expression (alone or with IL-6) was associated with or induced the expression of other “antimicrobial/regulatory” molecules such as S100A9 and Lcn-2.^{35–38}

Importantly, in several independent *in vivo* protocols where eTg/IL-6 macrophages and PAO1 were given sequentially, BAL cells and solutes showed a regulatory phenotype, as evidenced by downregulation of iNOS expression (Figure S4C), increased IL-10 (Figure S4D), IL-6, Lcn-2, and YM-1 (Figure 8) protein levels, and lymphocyte-inhibitory properties (Figure S5). This lung regulatory phenotype was independent of the presence of lymphocytes (Figure 6) and was confirmed by t-SNE and flow SOM FACS analysis. Indeed, we showed that the frequency of type I alveolar cells and the ratio of type I to type II cells was decreased by PAO1 infection, and was rescued in mice receiving elafin-IL-6 macrophages (Figure 7). Although we cannot rule out a “direct” protective effect on type I cells by elafin, whereby its anti-neutrophil elastase activity³⁹ would prevent sloughing of these



(legend on next page)

cells, the increased frequency of a EpCAM+ Ki-67+Sca-1+/- population in “elafin-IL-6 mice” (Figure 7) also demonstrates that the elafin-IL-6-modified macrophages endow the lung with a proliferative/repair phenotype, potentially (although not studied in depth here) through the stem-like properties of type II cells. This further demonstrates the usefulness of Sca-1 as a marker of *Pseudomonas*-induced alveolar repair^{17,40} and confirms that macrophages are able to promote epithelial proliferation.⁴¹

Importantly for potential therapeutic applications (see below), we demonstrated in kinetics experiments that transferred eTg-BMDMs could remain in the alveolar space for at least 2–3 weeks, without inducing any unwanted pro-inflammatory events. Indeed, since C57BL/6 mice do not express the elafin gene, the detection of the latter necessarily indicates the long-term presence of the transfected, adoptively transferred human gene (see corresponding Figure S9 and Supplemental results).

In conclusion, although approaches aiming at reinforcing the protection of the alveolar unit through AM-mediated therapy have been modeled, e.g., in genetic diseases such as alveolar proteinosis, primary immunodeficiency, or alpha-1-Pi deficiency,^{15,42–44} fewer efforts have been geared, as far as we are aware, toward acute infectious situations.^{15,45,46} Our study confirms the importance of lung epithelial cells in the defense against PAO1^{47,48} and shows for the first time that complementing AMs with a genetic IL-6-elafin combination provides AMs with a unique long-lasting new “M2-regulatory/antimicrobial” signature, which enhances epithelial cell proliferation and tissue repair (see Figure S10 for a schematic summary). We believe that this will have to be confirmed in a therapeutic study (in addition to the prophylactic setup presented here) and that this could be of value for treating acute bacterial infections in the lung, i.e., in ventilator-associated pneumonia and CF,^{1,49} or in lung exacerbations observed in chronic obstructive pulmonary disease (COPD).⁵⁰ Indeed, echoing this statement, recent innovative studies have also demonstrated the value of either hematopoietic stem cell transplantation in CF mice, in a *Pseudomonas aeruginosa* infectious setting,⁵¹ or that of adoptive transfers of macrophage progenitors or induced pluripotent stem cell-derived macrophages in alveolar proteinosis.^{52,53}

MATERIALS AND METHODS

In vivo experiments

Animals

Seven- to ten-week-old male C57BL/6 WT and age-matched eTg mice were purchased from Janvier Labs (Le Genest-Saint-Isle, France)

or generated by our group¹⁶ and bred in house, respectively. The latter has been backcrossed 11 times on the C57BL/6 background. Rag1, gamma c double KO mice were a gift from Dr J. Di Santo (Institut Pasteur, Paris, France). Animals were kept in a specific pathogen-free facility under 12-h light/dark cycles, with free access to food and water. Procedures were approved by our local ethical committee and by the French Ministry of Education and Research (agreement number 04537.03).

Macrophage adoptive transfer and PAO1 lung infection

Mice (WT-AM or eTg-AM) were anesthetized with intraperitoneal injection of 100 μ L of ketamine 500 and xylazine 2% in 0.9% NaCl (10:10:80). Primary AMs recovered by BAL (~100–150,000 per mouse) were infected for 6 h with adenovirus (multiplicity of infection [MOI] 25) Ad Null or Ad-IL-6 and left overnight. The next day, cells were detached with PBS-EDTA 0.5 mM and washed, and the cell pellet was re-suspended in 50 μ L of sterile PBS for adoptive transfer by intratracheal route through the oropharynx, with an air-filled syringe (500 μ L), as described previously.^{5,6}

When relevant, sub-lethal doses (5×10^6 CFU) or lethal doses of PAO1 were used for mechanistic or survival experiments, respectively. At various times, mice were then euthanized with pentobarbital, tracheae were cannulated, and a BAL (2 mL of total volume) was performed. BALF supernatant was kept at -80°C until further use, e.g., for cytokine/chemokine measurement, with DuoSet enzyme-linked immunosorbent assay (ELISA) kits (R&D Systems). Simultaneously, the BAL cell pellet was resuspended in 400 μ L of PBS for cell type analysis using cytospin centrifugation and Diff-Quik staining (Medion Diagnostics). In parallel, lungs were recovered in 1 mL of PBS and homogenized with a FastPrep-24 (MP Biomedicals) during two cycles (speed 6, 45 s). Homogenates were then used for cytokine/chemokine measurements or FACS analysis (see below).

Ex vivo experiments

Primary alveolar macrophages

Primary AMs were isolated from WT and eTg mice by BAL as described previously.⁶ BALFs were centrifuged (2,000 rpm, 10 min, 4°C), and cell pellets were re-suspended in RPMI-Glutamax (10% fetal calf serum [FCS], 1,000 U/mL penicillin, 100 μ g/mL streptomycin). Cells were cultured for 16 h (37°C , 5% CO_2) in 48-well Corning Costar culture plates (250,000 cells/well) prior to stimulation or infection.

Figure 7. t-SNE and flow SOM FACS analysis at the onset of lung repair (day 3 post-PAO1)

(A) Bone marrow-derived macrophages (BMDMs) were generated and pre-infected with Ad Null or Ad-mIL6 as described in the above figures. 1.5×10^6 BMDMs were transferred into WT mice, and 48 h after transfer mice were infected with a lower sub-lethal dose of PAO1 (5×10^5 CFU/mouse) and euthanized 3 days after infection (at the onset of lung repair). (B and C) FACS BMDM staining procedure was as described above, using podoplanin and SPC as markers of type I and type II pneumocytes, respectively. Data represent individual mice. Statistical significance: ANOVA, multiple comparison, Tukey's test, * $p < 0.05$; ** $p < 0.01$; *** $p < 0.001$; **** $p < 0.0001$. (D–H) With a t-distributed stochastic neighbor embedding (t-SNE) and self-organizing map (SOM) analysis (see Materials and methods), 70,000 random events, i.e., 8,750 per mouse \times 4 mice \times 2 groups (WT-Ad Null and eTg-IL-6) were analyzed with the tSNE script in FlowJo to create a 2-dimensional map (D) and a heatmap of all the markers used in the experiment (E). Further, 3 populations (Pops I–III) were identified whose frequencies were shown to be higher in the eTg-IL-6 group (F). Finally, we focused on the bigger population (Pop I, (G)) and analyzed the markers Ki-67, Podoplanin, Sca-1, EpCAM, SP-C, and CD45 in that population (H).

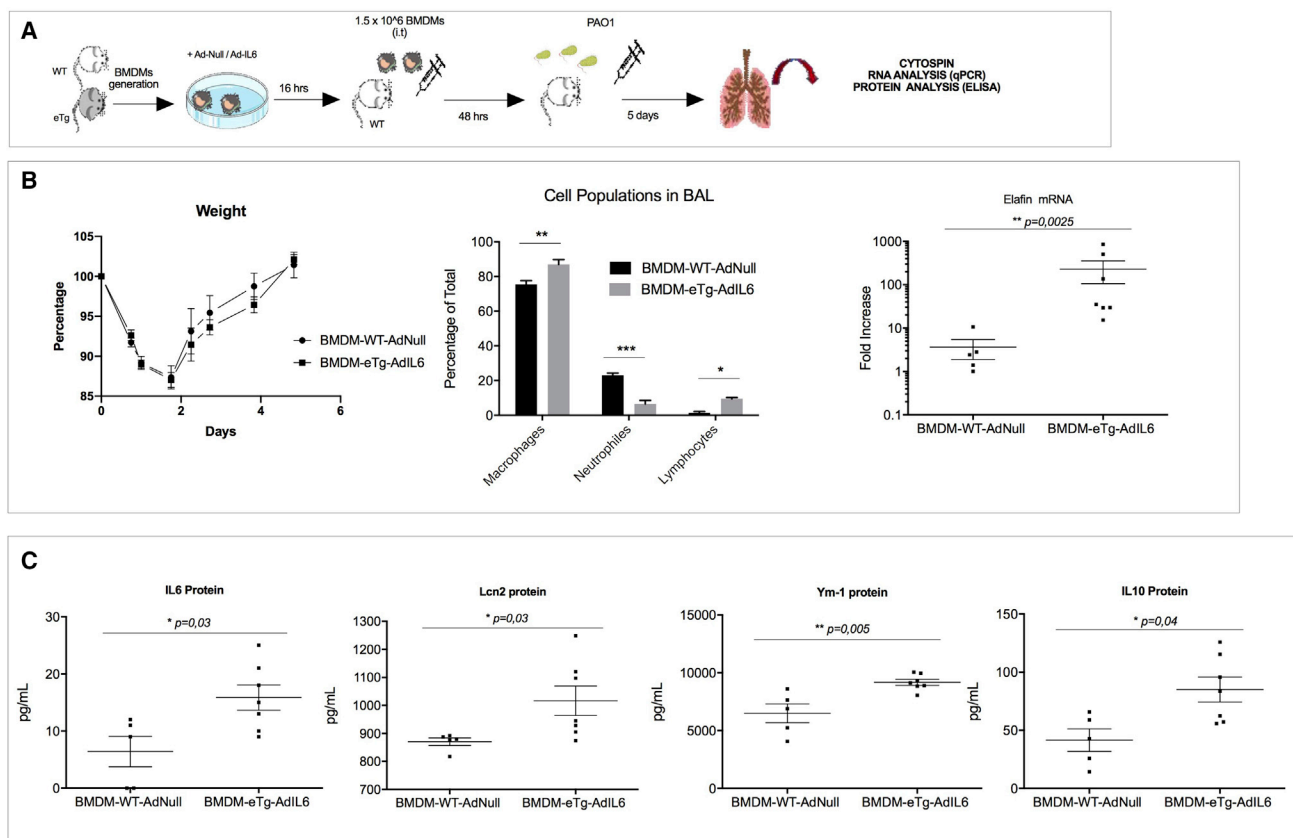


Figure 8. eTg-Ad-IL-6 regulatory phenotype at recovery (day 5 post-PAO1)

(A) Bone marrow-derived macrophages (BMDMs) were generated and pre-infected with Ad Null or Ad-IL6 as described in the above figures. 1.5×10^6 BMDMs were transferred into WT mice, and 48 h after transfer, mice were infected with a lower sub-lethal dose of PAO1 (5×10^5 CFU/mouse) and euthanized 5 days after infection, when mice recovered their initial weight. (B) Body weight was monitored daily after PAO1 infection (left). At day 5, BAL alveolar cells were counted from the performed cytopsin (middle). BALF pelleted cells were lysed, and Elafin mRNA expression was measured by qPCR. (C) Recovered BALs were centrifuged, and proteins were quantified in BALF by ELISA. Each point represents an individual mouse. Data show mean \pm SEM. Statistical significance: two-way ANOVA, multiple comparison, Tukey's test (B, middle), * $p < 0.05$; ** $p < 0.01$; *** $p < 0.001$; **** $p < 0.0001$; t tests with Bonferroni's post hoc (B, right and C).

Bone marrow-derived macrophage generation

Bone marrow was extracted from mice femurs, and cells were washed with PBS and centrifuged at 1,400 rpm for 7 min (4°C). Pelleted cells were then re-suspended with lysis buffer (Gibco) for 2 min at room temperature to lyse red blood cells. After another wash, cells were seeded in complete DMEM medium (10% FCS, 1,000 U/mL penicillin, 100 μ g/mL streptomycin) containing 30 ng/mL of mouse macrophage colony stimulating factor (M-CSF) (PeproTech). After two successive medium replacements (at day 3 and day 6), macrophages were detached, washed, and re-suspended in cold sterile PBS at day 9 and kept on ice before further use. For *in vitro* experiments, cells were seeded in 24-well culture plates (500,000 cells/well) in RPMI-Glutamax (10% FCS, 1,000 U/mL penicillin, 100 μ g/mL streptomycin) for 12 h prior to stimulation or infection. For *in vivo* adoptive transfer experiments, BMDM density was adjusted to 10^6 cells/50 μ L in sterile PBS before oropharyngeal instillation.

Total splenocyte proliferation assay

The spleen of a WT C57BL/6 mouse was harvested, processed, and homogenized into a single-cell suspension through mechanical disruption. Briefly, the spleen was grinded and filtered on a 40- μ m sterile filter. The filter was washed with DMEM-Glutamax (10% FCS, 1,000 U/mL penicillin, 100 μ g/mL streptomycin), and the recovered cells were centrifuged (2,000 rpm, 4°C). Pelleted cells were re-suspended for 5 min at room temperature with 1 mL of ACK Lysis buffer to lyse red blood cells. Lysis reaction was stopped by adding 30 mL of sterile PBS 1 \times , and cells were centrifuged (2,000 rpm, 4°C). Pelleted cells were re-suspended at 2×10^7 /mL in 37°C pre-warmed PBS and incubated for 10 min at 37°C with 2.5 μ M CFSE. Labeling was quenched with three washes of ice-cold DMEM-Glutamax (10% FCS, 1,000 U/mL penicillin, 100 μ g/mL streptomycin). The CFSE-labeled cells were seeded in a 96-well culture plate (10×10^4 cells/well) in DMEM-Glutamax (10% FCS, 1,000 U/mL penicillin, 100 μ g/mL streptomycin) supplemented with 30 U/mL of mouse

rIL-2. 2 μ L of Dynabeads Mouse T-Activator CD3/CD28 (Gibco Life Technologies) were added in each well except for a control well (negative control). 100 μ L of PBS (control) or BALF was then added into the wells, and cells were left in culture for 72 h. Cells were then harvested and washed with FACS buffer (PBS-1% FCS), and CFSE intensity was analyzed by flow cytometry.

***In vitro* experiments**

Alveolar epithelial cell lines

Mouse alveolar epithelial cell line CMT-2 (CMT64/61, European Collection of Authenticated Cell Cultures, ECACC) and mtCC-DJS2, an immortalized adult Clara cell line (Ref. S1, see [Supplemental references](#)), a kind gift from Dr. DeMayo (Baylor College of Medicine, Houston, TX, USA), were cultured in DMEM-Glutamax (10% FCS, 1,000 U/mL penicillin, 100 μ g/mL streptomycin). Cells were placed for 12 h (37°C, 5% CO₂) in 24-well Corning Costar culture plates (500,000 cells/well) prior to stimulation.

Alveolar macrophage cell line MPI

Alveolar macrophages MPI cells⁵⁴ were cultured in RPMI-Glutamax (10% FCS, 1,000 U/mL penicillin, 100 μ g/mL streptomycin) supplemented with 30 ng/ml GM-CSF (PeproTech). Cells were placed for 16 h (37°C, 5% CO₂) in 48-well Corning Costar culture plates (250,000 cells/well) prior to stimulation or infection.

BMDM and CMT-2/DJS-2 epithelial cell co-culture

Club cells and alveolar epithelial cells (DJS-2 and CMT-2 cell lines, respectively) were seeded in a 24-well plate (500,000 cells/well). A 12-mm-diameter Transwell insert of 0.4- μ m pore size containing 100,000 of either WT or eTg-BMDMs (pre-infected with Ad Null or Ad-mIL6) was placed in each insert, except for the non-treated control well (CTRL). After 16 h, BMDMs were either mock-treated or infected with WT PAO1 (MOI 0.5) for 6 h. Epithelial cells were then lysed, and antimicrobial peptide/cytokine mRNA expression levels were determined by quantitative RT-PCR.

Localization of Elafin to the nucleus

5×10^5 MPI cells were seeded in 24-well plates containing 0.5 mL of complete RPMI medium (10% FCS, 1% Pen/Strep) and left overnight. The next day, cells were PBS washed and incubated with increasing concentrations (0.4 μ M, 2 μ M, 4 μ M) of full length (FL)-elafin or T2-elafin (see below, [Supplemental results](#), and [Figure S3](#)) in serum-free RPMI medium for 1 h. At the end of the experiment, cells were lysed and subcellular protein fractionation was performed with the NE-PER Nuclear and Cytoplasmic Extraction Reagents (Thermo Scientific). Cytoplasmic and nuclear Elafin concentrations were determined by ELISA.

Binding of T2-Elafin to DNA

Briefly, 40 mg of cellulose beads coupled to double-stranded calf thymus DNA (Sigma-Aldrich, D8515) were incubated with 20 μ g of T2-Elafin for 1 h at 4°C in incubation buffer (20 mM Tris, 100 mM potassium chloride, 1 mM EDTA, 10% glycerol, 1 mM DTT, 1 mg/mL BSA, 0.2% Triton X-100, pH 7.5). Beads were then

centrifuged for 2 min at 3,000 rpm and washed twice in wash buffer (20 mM Tris, 110 mM potassium acetate, 1 mM EDTA, 10% glycerol, 1 mg/mL BSA, 0.2% Triton X-100, pH 7.5). T2-Elafin was eluted with increasing concentrations of elution buffer (PBS-NaCl 0.15 M up to 1.5 M). Elafin concentration was determined in the eluate by ELISA.

Binding of Elafin to IL-6 promoter

MPI cells were seeded in 24-well plates containing 0.5 mL of complete RPMI medium (10% FCS, 1% Pen/Strep) and were either mock-treated or infected with either Ad Null or Ad-Elafin at a MOI of 25. Alternatively, cells were treated with increasing quantities of full-length elafin (T2, obtained commercially [R&D Systems]) or with chemically synthesized (LPS free) elafin moieties, namely, the full-length (FL) 95-aa molecule (with a net cationic charge of +7 and active as an anti-protease [Refs. S2 and S3, see [Supplemental references](#)]), the C terminus (aa 38-95 of FL-elafin, with a net cationic charge of +3 and active as an anti-protease), or the N terminus (aa 1-50 of FL-elafin, with a net cationic charge of +5 and inactive as an anti-protease). After an overnight incubation, cells were further transfected with 1 μ g of plasmid DNA coding for the luciferase gene driven by the IL-6 promoter (pmIL-6 FL (fly luciferase) #61286-, Addgene), diluted into 0.25 mL of Opti-MEM medium, to which 0.25 mL of Opti-MEM 3% Lipofectamine 2000 was added. After 6 h, cells were washed and replenished with complete RPMI medium overnight. 16 h later, cells were washed again and were either mock-treated or infected with PAO1 (MOI 1) for 5 h in serum-free RPMI. At the end of the experiment, cells were lysed for assessment of RLI:luciferase activity (Promega kit) and supernatants were used to measure cytokine release.

Vectors and bacteria

Adenovirus constructs and adenovirus infection

The control Ad Null,⁵⁵ Ad-mIL6,⁵⁶ and Ad-hElafin⁵⁷ constructs are replication-deficient Ad vectors. The latter two were used to transiently overexpress murine IL-6 and human elafin.

Cells (AMs, BMDMs, and MPI) were washed 3 times with sterile PBS and infected for 6 h with the different Ad constructs with a MOI of 25 in serum-free RPMI-Glutamax. The wells were washed, and cells were placed overnight in serum- and antibiotic-free fresh RPMI-Glutamax prior to further stimulation, infection with PAO1, or adoptive transfer.

Pseudomonas aeruginosa O1 strain, macrophage infection, and bacterial clearance measurement

PAO1 strain (ATCC 15692) was kept in freezing medium (50% Luria broth [LB], 50% glycerol) and stored at -80°C until use. Before infection experiments, PAO1 strain was grown overnight in LB in a rotating incubator (200 rpm, 37°C). The bacterial suspension was then diluted in serum- and antibiotic-free RPMI medium, and the optical density (OD) was measured at 600 nm every 2 h until logarithmic growth phase was reached ($0.1 < \text{OD} < 0.3$; an OD of 0.1 is equivalent to a bacterial concentration of 7.7×10^7 CFU/mL).

Table 1. FACS antibodies

Antibody	Fluorochrome	Dilution	Isotype	Clone	Manufacturer
Fixable viability dye	eFluor 506	1/500			eBioscience
CD16/CD32		1/100	rat IgG2a, λ	93	BioLegend
CD45	Pe-Cy7	1/400	rat IgG2b, κ	30-F11	BioLegend
CD11b	PerCP/Cy5	1/400	rat IgG2b, κ	M1/70	BioLegend
CD11c	Pacific Blue	1/400	American hamster IgG	N418	BioLegend
F4/80	PE/Dazzle 594	1/400	rat IgG2a, κ	BM8	BioLegend
IA/IE	BV605	1/600	rat IgG2b, κ	M5/114.15.2	BioLegend
Ly6C	APC/Cyanine 7	1/100	rat IgG2c, κ	HK1.4	BioLegend
Ly6G	Alexa Fluor 700	1/100	rat IgG2a, κ	1A8	BioLegend
IL4Ra	PE	1/100	Lewis IgG2a, κ	E50-2440	BD Biosciences
SiglecF	BV711	1/200	rat IgG2a, κ	E50-2440	BD Biosciences
h/m Arg-1	PE	1/50	sheep IgG		R & D Systems
iNOS	Alexa Fluor 488	1/50	rabbit IgG		Cell Signaling Technology

IgG, immunoglobulin G.

Macrophages were either mock-treated or infected with either Ad Null, Ad-IL-6, or Ad-Elafin as explained above. Then, cells were infected with PAO1 for 4–6 h. Cell lysates and supernatants were then prepared for RNA or protein analysis (ELISA), respectively. Alternatively, clearance of bacteria was measured.⁶ Briefly, 10^5 macrophages were infected with PAO1 (MOI = 1) for 4 h in 96-well plates and cultured in RPMI medium (200 μ L/well), as indicated above. In parallel, “control wells (C well)” (with no macrophages) were set up to determine the baseline bacterial growth during 4 h. At the end of the experiment, supernatants (S) (0.2 mL diluted with 1.4 mL of PBS) were added to the cell layer (L), already lysed with 400 μ L of PBS containing 0.1% Triton X-100. Remaining bacteria were then counted in L + S as above on LB-agar plates. Bacterial killing was calculated by counting the remaining CFU in L + S at 4 h and normalized to the CFU obtained when the inoculum was seeded at T0 in the absence of macrophages. A value of 1 was given to the maximal bacterial clearance obtained with the WT strain of PAO1, and other treatments were then expressed relative to 1. When suitable, bacterial loading was assessed in lungs by qPCR, using the *P.a* oPRL gene as reference, as described previously⁵⁸ and as also validated previously in our hands.⁵⁹

RNA extraction, reverse transcription, and qPCR

RNA isolation from cells was performed with the PureLink RNA Mini Kit (12183018A, Ambion, Life Technologies), following the manufacturer’s instructions, and as described previously.⁶

qPCR primers were m18S: F: 5'-CTTAGAGGGACAAGTGGCG-3', R: 5'-ACGCTGAGCCAGTCAGTGTA-3'; mTNF: F: 5'-AGCCGA TGGGTTGTACCTT-3', R: 5'-CAGGGTAATGAGTGGGTTGG-3'; mLcn2: F: 5'-CCAGTTCGCCATGGTATTTT-3', R: 5'-CCAGTTC GCCATGGTATTTT-3'; mS100A9: F: 5'-AAAGGCTGTGGGAAGT AATTAAGA-3', R: 5'-GCCATTGAGTAAGCCATTTCC-3'; mLIL-1

β : F: 5'-ATGCCACCTTTTGACAGTGATG-3', R: 5'-GCTCTTGT TGATGTGCTGCT-3'; mLIL-6: F: 5'-GCACCAAGACCATCCAA TTC-3', R: 5'-ACCACAGTGAGGAATGTCCA-3'; mLIL-10: F: 5'-AAGGCAGTGGAGCAGGTGAA-3', R: 5'-CCAGCAGACTCAAT ACACAC-3'; mLIL-22: F: 5'-TTCCAGCAGCCATACATCGTC-3', R: 5'-TCGGAACAGTTTCTCCCG-3'; mLIL-23: F: 5'-AATCTCTG CATGCTAGCCTGG-3', R: 5'-GATTCATATGTCCCCTGGTG-3'; mYM-1: F: 5'-CACGGCACCTCTAAATTGT-3', R: 5'-CAGGG TAATGAGTGGGTTGG-3'; h-elafin: F: 5'-GGCTCCTGCCCAT TATCT-3', R: 5'-TCTTTCAAGCAGCGGTTAGG-3'.

Flow cytometry analysis

Classical analysis

C57BL/6 mouse lung epithelial cell preparation was as described in Raoust et al.⁶⁰ For FACS analysis, cells (from lung extracts, BALs, isolated AMs or BMDMs) were first incubated (10 min, 4°C) with a cocktail of a viability dye and Fc Block antibody. Cells were washed (2,000 rpm, 5 min) with FACS buffer (PBS-2% FCS) and then incubated (30 min, 4°C) with a cocktail of cell surface conjugated antibodies. For intracellular staining, cells were then permeabilized and stained with eBioscience Foxp3 Transcription Factor Staining Buffer Set according to the manufacturer’s protocol. Finally, cells were washed, and the pellets were re-suspended in FACS buffer for data acquisition. Data were acquired the same day with a LSRFortessa cytometer (BD Biosciences) with BD FACSDiva software and analyzed with FlowJo (Tree Star, Ashland, OR, USA). The antibodies used for FACS analysis are listed in Table 1.

Dimensionality reduction (t-SNE) analysis

A subset of 8,750 cells were selected for each mouse at random with the DownSampleV3 FlowJo plugin and merged into a single FCS file prior to t-SNE analysis. The following channels were removed from the expression matrix to only include protein markers in t-SNE

analysis: event length, viability, FSC, SSC, offset, residual, and time. A total of 70,000 cells and 6 markers were used to create the t-SNE map.

The dimensionality reduction algorithm was applied using the Barnes-Hut implementation with 1,000 iterations, a perplexity parameter of 30, and a trade-off θ of 0.5. The t-SNE map was generated by plotting each event by its t-SNE dimensions in a dot plot. Intensities for markers of interest were overlaid on the dot plot to show the expression of those markers on different cell islands and facilitate assignment of cell subsets to these islands.

Statistical analysis

Data were analyzed with GraphPad Prism Software 6.03. Statistical analysis was performed with either a non-parametric test (Kruskal-Wallis and Dunn's posttest) or one-way or two-way ANOVA followed by the appropriate multi-comparison post hoc Tukey's test.

Survival curves in murine model experiments were plotted with Kaplan-Meier curves, and statistical testing was performed with the log-rank (Mantel-Cox) test.

Differences were considered statistically significant when p was <0.05 and are labeled as follows: * $p < 0.05$; ** $p < 0.01$; *** $p < 0.001$; **** $p < 0.0001$.

SUPPLEMENTAL INFORMATION

Supplemental information can be found online at <https://doi.org/10.1016/j.ymthe.2021.08.007>.

ACKNOWLEDGMENTS

We wish to thank "Vaincre la Mucoviscidose" for recurrent support. S.K. was supported by the Labex "Inflamex" (PhD Grant G11003HH).

AUTHOR CONTRIBUTIONS

S.K. performed experiments and analyzed data. B.V. helped in performing some experiments. I.G.-V. helped in the design of the experiments and critically appraised a draft of the document. J.-M.S. designed experiments, analyzed data, and wrote the manuscript.

DECLARATION OF INTERESTS

The authors declare no competing interests.

REFERENCES

- Edelman, A., and Sallenave, J.-M. (2014). Cystic fibrosis, a multi-systemic mucosal disease: 25 years after the discovery of CFTR. *Int. J. Biochem. Cell Biol.* 52, 2–4.
- Sallenave, J.-M. (2014). Phagocytic and signaling innate immune receptors: are they dysregulated in cystic fibrosis in the fight against *Pseudomonas aeruginosa*? *Int. J. Biochem. Cell Biol.* 52, 103–107.
- Oliver, A., Mulet, X., López-Causapé, C., and Juan, C. (2015). The increasing threat of *Pseudomonas aeruginosa* high-risk clones. *Drug Resist. Updat.* 21–22, 41–59.
- Willyard, C. (2017). The drug-resistant bacteria that pose the greatest health threats. *Nature* 543, 15.
- Saint-Criq, V., Villeret, B., Bastaert, F., Kheir, S., Hatton, A., Cazes, A., Xing, Z., Sermet-Gaudelus, I., Garcia-Verdugo, I., Edelman, A., and Sallenave, J.M. (2018). *Pseudomonas aeruginosa* LasB protease impairs innate immunity in mice and humans by targeting a lung epithelial cystic fibrosis transmembrane regulator-IL-6 anti-microbial-repair pathway. *Thorax* 73, 49–61.
- Bastaert, F., Kheir, S., Saint-Criq, V., Villeret, B., My-Chan Dang, P., El-Benna, J., Sirard, J.C., Voulhoux, R., and Sallenave, J.M. (2018). *Pseudomonas aeruginosa* LasB Subverts Alveolar Macrophage Activity by Interfering With Bacterial Killing Through Downregulation of Innate Immune Defense, Reactive Oxygen Species Generation, and Complement Activation. *Front. Immunol.* 9, 1675.
- De Ravin, S.S., Wu, X., Moir, S., Anaya-O'Brien, S., Kwatema, N., Little, P., Theobald, N., Choi, U., Su, L., Marquesen, M., et al. (2016). Lentiviral hematopoietic stem cell gene therapy for X-linked severe combined immunodeficiency. *Sci. Transl. Med.* 8, 335ra57.
- Poletti, V., Charrier, S., Corre, G., Gjata, B., Vignaud, A., Zhang, F., Rothe, M., Schambach, A., Gaspar, H.B., Thrasher, A.J., and Mavilio, F. (2018). Preclinical Development of a Lentiviral Vector for Gene Therapy of X-Linked Severe Combined Immunodeficiency. *Mol. Ther. Methods Clin. Dev.* 9, 257–269.
- Vannucci, L., Lai, M., Chiappesi, F., Ceccherini-Nelli, L., and Pistello, M. (2013). Viral vectors: a look back and ahead on gene transfer technology. *New Microbiol.* 36, 1–22.
- Gordon, S.B., and Read, R.C. (2002). Macrophage defences against respiratory tract infections. *Br. Med. Bull.* 61, 45–61.
- Hussell, T., and Bell, T.J. (2014). Alveolar macrophages: plasticity in a tissue-specific context. *Nat. Rev. Immunol.* 14, 81–93.
- Kooguchi, K., Hashimoto, S., Kobayashi, A., Kitamura, Y., Kudoh, I., Wiener-Kronish, J., and Sawa, T. (1998). Role of alveolar macrophages in initiation and regulation of inflammation in *Pseudomonas aeruginosa* pneumonia. *Infect. Immun.* 66, 3164–3169.
- Allard, B., Panariti, A., and Martin, J.G. (2018). Alveolar Macrophages in the Resolution of Inflammation, Tissue Repair, and Tolerance to Infection. *Front. Immunol.* 9, 1777.
- Suzuki, T., Arumugam, P., Sakagami, T., Lachmann, N., Chalk, C., Sallase, A., Abe, S., Trapnell, C., Carey, B., Moritz, T., et al. (2014). Pulmonary macrophage transplantation therapy. *Nature* 514, 450–454.
- Ackermann, M., Kempf, H., Hetzel, M., Hesse, C., Hashtchin, A.R., Brinkert, K., Schott, J.W., Haake, K., Kühnel, M.P., Glage, S., et al. (2018). Bioreactor-based mass production of human iPSC-derived macrophages enables immunotherapies against bacterial airway infections. *Nat. Commun.* 9, 5088.
- Sallenave, J.-M., Cunningham, G.A., James, R.M., McLachlan, G., and Haslett, C. (2003). Regulation of pulmonary and systemic bacterial lipopolysaccharide responses in transgenic mice expressing human elafin. *Infect. Immun.* 71, 3766–3774.
- Liu, Y., Kumar, V.S., Zhang, W., Rehman, J., and Malik, A.B. (2015). Activation of type II cells into regenerative stem cell antigen-1(+) cells during alveolar repair. *Am. J. Respir. Cell Mol. Biol.* 53, 113–124.
- Dobbs, L.G., Williams, M.C., and Gonzalez, R. (1988). Monoclonal antibodies specific to apical surfaces of rat alveolar type I cells bind to surfaces of cultured, but not freshly isolated, type II cells. *Biochim. Biophys. Acta* 970, 146–156.
- McElroy, M.C., and Kasper, M. (2004). The use of alveolar epithelial type I cell-selective markers to investigate lung injury and repair. *Eur. Respir. J.* 24, 664–673.
- Lenssen, J., and Stolk, J. (2007). Pulmonary stem cells and the induction of tissue regeneration in the treatment of emphysema. *Int. J. Chron. Obstruct. Pulmon. Dis.* 2, 131–139.
- Berthiaume, Y., Lesur, O., and Dagenais, A. (1999). Treatment of adult respiratory distress syndrome: plea for rescue therapy of the alveolar epithelium. *Thorax* 54, 150–160.
- Bals, R., and Hiemstra, P.S. (2004). Innate immunity in the lung: how epithelial cells fight against respiratory pathogens. *Eur. Respir. J.* 23, 327–333.
- Descamps, D., Le Gars, M., Balloy, V., Barbier, D., Maschalidi, S., Tohme, M., Chignard, M., Ramphal, R., Manoury, B., and Sallenave, J.M. (2012). Toll-like receptor 5 (TLR5), IL-1 β secretion, and asparagine endopeptidase are critical factors for alveolar macrophage phagocytosis and bacterial killing. *Proc. Natl. Acad. Sci. USA* 109, 1619–1624.
- Rubins, J.B. (2003). Alveolar macrophages: wielding the double-edged sword of inflammation. *Am. J. Respir. Crit. Care Med.* 167, 103–104.
- Westphalen, K., Gusarova, G.A., Islam, M.N., Subramanian, M., Cohen, T.S., Prince, A.S., and Bhattacharya, J. (2014). Sessile alveolar macrophages communicate with alveolar epithelium to modulate immunity. *Nature* 506, 503–506.

26. Morris, D.G., Huang, X., Kaminski, N., Wang, Y., Shapiro, S.D., Dolganov, G., Glick, A., and Sheppard, D. (2003). Loss of integrin $\alpha(v)\beta6$ -mediated TGF- β activation causes Mmp12-dependent emphysema. *Nature* 422, 169–173.
27. Taggart, C.C., Cryan, S.A., Weldon, S., Gibbons, A., Greene, C.M., Kelly, E., Low, T.B., O'Neill, S.J., and McElvaney, N.G. (2005). Secretory leucoprotease inhibitor binds to NF-kappaB binding sites in monocytes and inhibits p65 binding. *J. Exp. Med.* 202, 1659–1668.
28. Xing, Z., Gaudie, J., Cox, G., Baumann, H., Jordana, M., Lei, X.F., and Achong, M.K. (1998). IL-6 is an antiinflammatory cytokine required for controlling local or systemic acute inflammatory responses. *J. Clin. Invest.* 101, 311–320.
29. Scheller, J., Chalaris, A., Schmidt-Arras, D., and Rose-John, S. (2011). The pro- and anti-inflammatory properties of the cytokine interleukin-6. *Biochim. Biophys. Acta* 1813, 878–888.
30. Dubey, A., Izakelian, L., Ayaub, E.A., Ho, L., Stephenson, K., Wong, S., Kwofie, K., Austin, R.C., Botelho, F., Ask, K., and Richards, C.D. (2018). Separate roles of IL-6 and oncostatin M in mouse macrophage polarization in vitro and in vivo. *Immunol. Cell Biol.* 96, 257–272.
31. Fernando, M.R.J.L., Reyes, J.L., Iannuzzi, J., Leung, G., and McKay, D.M. (2014). The pro-inflammatory cytokine, interleukin-6, enhances the polarization of alternatively activated macrophages. *PLoS ONE* 9, e94188.
32. Mauer, J., Chaurasia, B., Goldau, J., Vogt, M.C., Ruud, J., Nguyen, K.D., Theurich, S., Hausen, A.C., Schmitz, J., Brönneke, H.S., et al. (2014). Signaling by IL-6 promotes alternative activation of macrophages to limit endotoxemia and obesity-associated resistance to insulin. *Nat. Immunol.* 15, 423–430.
33. Braune, J., Weyer, U., Hobusch, C., Mauer, J., Brüning, J.C., Bechmann, I., and Gericke, M. (2017). IL-6 Regulates M2 Polarization and Local Proliferation of Adipose Tissue Macrophages in Obesity. *J. Immunol.* 198, 2927–2934.
34. Biswas, A., Bhattacharya, A., Kar, S., and Das, P.K. (2011). Expression of IL-10-triggered STAT3-dependent IL-4R α is required for induction of arginase 1 in visceral leishmaniasis. *Eur. J. Immunol.* 41, 992–1003.
35. Chan, Y.R., Liu, J.S., Pociask, D.A., Zheng, M., Mietzner, T.A., Berger, T., Mak, T.W., Clifton, M.C., Strong, R.K., Ray, P., and Kolls, J.K. (2009). Lipocalin 2 is required for pulmonary host defense against Klebsiella infection. *J. Immunol.* 182, 4947–4956.
36. Wang, Y., Jia, M., Yan, X., Cao, L., Barnes, P.J., Adcock, I.M., Huang, M., and Yao, X. (2017). Increased neutrophil gelatinase-associated lipocalin (NGAL) promotes airway remodelling in chronic obstructive pulmonary disease. *Clin. Sci. (Lond.)* 131, 1147–1159.
37. Rahimi, S., Roushandeh, A.M., Ebrahimi, A., Samadani, A.A., Kuwahara, Y., and Roudkenar, M.H. (2019). CRISPR/Cas9-mediated knockout of Lcn2 effectively enhanced CDDP-induced apoptosis and reduced cell migration capacity of PC3 cells. *Life Sci.* 231, 116586.
38. Parmar, T., Parmar, V.M., Perusek, L., Georges, A., Takahashi, M., Crabb, J.W., and Maeda, A. (2018). Lipocalin 2 Plays an Important Role in Regulating Inflammation in Retinal Degeneration. *J. Immunol.* 200, 3128–3141.
39. Sallenave, J.M., and Ryle, A.P. (1991). Purification and characterization of elastase-specific inhibitor. Sequence homology with mucus proteinase inhibitor. *Biol. Chem. Hoppe Seyler* 372, 13–21.
40. Liu, Y., Sadikot, R.T., Adami, G.R., Kalinichenko, V.V., Pendyala, S., Natarajan, V., Zhao, Y.Y., and Malik, A.B. (2011). FoxM1 mediates the progenitor function of type II epithelial cells in repairing alveolar injury induced by *Pseudomonas aeruginosa*. *J. Exp. Med.* 208, 1473–1484.
41. Hung, L.Y., Sen, D., Oniskey, T.K., Katzen, J., Cohen, N.A., Vaughan, A.E., Nieves, W., Urisman, A., Beers, M.F., Krummel, M.F., and Herbert, D.R. (2019). Macrophages promote epithelial proliferation following infectious and non-infectious lung injury through a Trefoil factor 2-dependent mechanism. *Mucosal Immunol.* 12, 64–76.
42. Wu, M., Hussain, S., He, Y.H., Pasula, R., Smith, P.A., and Martin, W.J., 2nd (2001). Genetically engineered macrophages expressing IFN-gamma restore alveolar immune function in scid mice. *Proc. Natl. Acad. Sci. USA* 98, 14589–14594.
43. Zhang, D., Wu, M., Nelson, D.E., Pasula, R., and Martin, W.J., 2nd (2003). Alpha-1-antitrypsin expression in the lung is increased by airway delivery of gene-transfected macrophages. *Gene Ther.* 10, 2148–2152.
44. Doerschuk, C.M. (2015). Pulmonary alveolar proteinosis and macrophage transplantation. *N. Engl. J. Med.* 372, 1762–1764.
45. D'Alessio, F.R., Craig, J.M., Singer, B.D., Files, D.C., Mock, J.R., Garibaldi, B.T., Fallica, J., Tripathi, A., Mandke, P., Gans, J.H., et al. (2016). Enhanced resolution of experimental ARDS through IL-4-mediated lung macrophage reprogramming. *Am. J. Physiol. Lung Cell. Mol. Physiol.* 310, L733–L746.
46. Shirey, K.A., Pletneva, L.M., Puche, A.C., Keegan, A.D., Prince, G.A., Blanco, J.C., and Vogel, S.N. (2010). Control of RSV-induced lung injury by alternatively activated macrophages is IL-4R alpha-, TLR4-, and IFN-beta-dependent. *Mucosal Immunol.* 3, 291–300.
47. Leiva-Juárez, M.M., Kolls, J.K., and Evans, S.E. (2018). Lung epithelial cells: therapeutically inducible effectors of antimicrobial defense. *Mucosal Immunol.* 11, 21–34.
48. Cleaver, J.O., You, D., Michaud, D.R., Pruneda, F.A., Juarez, M.M., Zhang, J., Weill, P.M., Adachi, R., Gong, L., Moghaddam, S.J., et al. (2014). Lung epithelial cells are essential effectors of inducible resistance to pneumonia. *Mucosal Immunol.* 7, 78–88.
49. Oliver, A., Cantón, R., Campo, P., Baquero, F., and Blázquez, J. (2000). High frequency of hypermutable *Pseudomonas aeruginosa* in cystic fibrosis lung infection. *Science* 288, 1251–1254.
50. Rakhimova, E., Wiehlmann, L., Brauer, A.L., Sethi, S., Murphy, T.F., and Tümmler, B. (2009). *Pseudomonas aeruginosa* population biology in chronic obstructive pulmonary disease. *J. Infect. Dis.* 200, 1928–1935.
51. Brinkert, K., Hedtfeld, S., Burhop, A., Gastmeier, R., Gad, P., Wedekind, D., Kloth, C., Rothschild, J., Lachmann, N., Hetzel, M., et al. (2021). Rescue from *Pseudomonas aeruginosa* airway infection via stem cell transplantation. *Mol. Ther.* 29, 1324–1334.
52. Happle, C., Lachmann, N., Ackermann, M., Mirenska, A., Göhring, G., Thomay, K., Mucci, A., Hetzel, M., Glomb, T., Suzuki, T., et al. (2018). Pulmonary Transplantation of Human Induced Pluripotent Stem Cell-derived Macrophages Ameliorates Pulmonary Alveolar Proteinosis. *Am. J. Respir. Crit. Care Med.* 198, 350–360.
53. Happle, C., Lachmann, N., Škuljec, J., Wetzke, M., Ackermann, M., Brenning, S., Mucci, A., Jirmo, A.C., Groos, S., Mirenska, A., et al. (2014). Pulmonary transplantation of macrophage progenitors as effective and long-lasting therapy for hereditary pulmonary alveolar proteinosis. *Sci. Transl. Med.* 6, 250ra113.
54. Fejer, G., Wegner, M.D., Györy, I., Cohen, I., Engelhard, P., Voronov, E., Manke, T., Ruzsics, Z., Dölken, L., Prazeres da Costa, O., et al. (2013). Nontransformed, GM-CSF-dependent macrophage lines are a unique model to study tissue macrophage functions. *Proc. Natl. Acad. Sci. USA* 110, E2191–E2198.
55. Bett, A.J., Haddara, W., Prevec, L., and Graham, F.L. (1994). An efficient and flexible system for construction of adenovirus vectors with insertions or deletions in early regions 1 and 3. *Proc. Natl. Acad. Sci. USA* 91, 8802–8806.
56. Braciak, T.A., Mittal, S.K., Graham, F.L., Richards, C.D., and Gaudie, J. (1993). Construction of recombinant human type 5 adenoviruses expressing rodent IL-6 genes. An approach to investigate in vivo cytokine function. *J. Immunol.* 151, 5145–5153.
57. Sallenave, J.-M., Xing, Z., Simpson, A.J., Graham, F.L., and Gaudie, J. (1998). Adenovirus-mediated expression of an elastase-specific inhibitor (elafin): a comparison of different promoters. *Gene Ther.* 5, 352–360.
58. Le Gall, F., Le Berre, R., Rosec, S., Hardy, J., Gouriou, S., Boisramé-Gastrin, S., Vallet, S., Rault, G., Payan, C., and Héry-Arnaud, G. (2013). Proposal of a quantitative PCR-based protocol for an optimal *Pseudomonas aeruginosa* detection in patients with cystic fibrosis. *BMC Microbiol.* 13, 143.
59. Villeret, B., Solhonne, B., Straube, M., Lemaire, F., Cazes, A., Garcia-Verdugo, I., and Sallenave, J.M. (2020). *Influenza A Virus Pre-Infection Exacerbates Pseudomonas aeruginosa-Mediated Lung Damage Through Increased MMP-9 Expression, Decreased Elafin Production and Tissue Resilience.* *Front. Immunol.* 11, 117.
60. Raoust, E., Balloy, V., Garcia-Verdugo, I., Touqui, L., Ramphal, R., and Chignard, M. (2009). *Pseudomonas aeruginosa* LPS or flagellin are sufficient to activate TLR-dependent signaling in murine alveolar macrophages and airway epithelial cells. *PLoS ONE* 4, e7259.